Acta Pharmaceutica Sinica B 2024;14(11):4789–4805

Chinese Pharmaceutical Association
Institute of Materia Medica, Chinese Academy of Medical Sciences

Acta Pharmaceutica Sinica B

www.elsevier.com/locate/apsb
www.sciencedirect.com

ORIGINAL ARTICLE

GPR17 modulates anxiety-like behaviors *via* basolateral amygdala to ventral hippocampal CA1 glutamatergic projection

Ruizhe Nie, Xinting Zhou, Jiaru Fu, Shanshan Hu, Qilu Zhang, Weikai Jiang, Yizi Yan, Xian Cao, Danhua Yuan, Yan Long, Hao Hong*, Susu Tang*

Department of Pharmacology, College of Pharmacy, China Pharmaceutical University, Nanjing 211198, China

Received 25 March 2024; received in revised form 17 June 2024; accepted 26 July 2024

KEY WORDS

GPR17;
CRS;
Anxiety;
Basolateral amygdala;
Ventral hippocampal CA1;
Glutamatergic neurons;
Glutamatergic projection;
Cangrelor

Abstract Anxiety disorders are one of the most epidemic and chronic psychiatric disorders. An incomplete understanding of anxiety pathophysiology has limited the development of highly effective drugs against these disorders. GPR17 has been shown to be involved in multiple sclerosis and some acute brain injury disorders. However, no study has investigated the role of GPR17 in psychiatric disorders. In a well-established chronic restraint stress (CRS) mouse model, using a combination of pharmacological and molecular biology techniques, viral tracing, *in vitro* electrophysiology recordings, *in vivo* fiber photometry, chemogenetic manipulations and behavioral tests, we demonstrated that CRS induced anxiety-like behaviors and increased the expression of GPR17 in basolateral amygdala (BLA) glutamatergic neurons. Inhibition of GPR17 by cangrelor or knockdown of GPR17 by adeno-associated virus in BLA glutamatergic neurons effectively improved anxiety-like behaviors. Overexpression of GPR17 in BLA glutamatergic neurons increased the susceptibility to anxiety-like behaviors. What's more, BLA glutamatergic neuronal activity was required for anxiolytic-like effects of GPR17 antagonist and GPR17 modulated anxiety-like behaviors *via* BLA to ventral hippocampal CA1 glutamatergic projection. Our study finds for the first and highlights the new role of GPR17 in regulating anxiety-like behaviors and it might be a novel potential target for therapy of anxiety disorders.

*Corresponding authors.
E-mail addresses: honghao@cpu.edu.cn (Hao Hong), tang_susu@126.com (Susu Tang).

Peer review under the responsibility of Chinese Pharmaceutical Association and Institute of Materia Medica, Chinese Academy of Medical Sciences.

https://doi.org/10.1016/j.apsb.2024.08.005

1. Introduction

Anxiety disorders are one of the most epidemic and chronic psychiatric disorders, such as generalized anxiety disorder, social anxiety disorder, panic disorder and agoraphobia[1-3]. Anxiety disorders are related to increasing economic burdens for society and families and reduce the quality of life for individuals. However, due to unclear etiology and pathogenesis, there has been no substantial breakthrough in the development of anxiolytic drugs in recent years. Currently, the first-line pharmacological treatment for most anxiety disorders is antidepressants, including selective serotonin reuptake inhibitors and serotonin noradrenaline reuptake inhibitors[4]. Unfortunately, these drugs have some disadvantages such as slow onset, low efficacy, and significant adverse reactions, greatly reducing patients' medication compliance. Therefore, exploring new targets of anxiolytics is urgently needed to treat anxiety disorders more effectively.

GPR17 is a G-protein coupled receptor (GPCR), lacks defined ligands, but responds to both nucleotide sugars and cysteinyl leukotrienes which are two unrelated families of endogenous ligands[5-7]. In our previous studies, we found that cysteinyl leukotrienes and their receptors, particularly cysteinyl leukotrienes receptors 1 are involved in regulating neurological and psychiatric disorders such as Alzheimer's disease and depression[8-12]. Importantly, GPR17, as one of the receptors that could be activated by cysteinyl leukotrienes, is highly expressed in the central nervous system, especially oligodendrocytes and neurons, whereas it is not expressed in astrocytes[13]. Numerous researches have depicted that GPR17 is predominantly located in oligodendrocyte cells of healthy brains and plays a stage-specific role in the differentiation and maturation of oligodendrocyte precursor cells[14-17]. It has been generally acknowledged that GPR17 is a candidate target to treat the diseases of spinal cord injury, multiple sclerosis and stroke[18-22]. In addition, some studies have reported that GPR17 is highly expressed in neurons of ischemic and traumatic brains, and is considered as a damage sensor to regulate acute neuronal injury and late microgliosis[23-27]. However, no studies have investigated the function and neuron types expressing of GPR17 in psychiatric disorders. Since anxiety disorders are the most common psychiatric disorders, we intend to explore the role of GPR17 in anxiety disorders.

In the present experiments, we applied a chronic restraint stress model in which mice are induced anxiety-like behaviors[28-31]. Using a combination of pharmacological and molecular biology techniques, viral tracing, *in vitro* electrophysiology recordings, *in vivo* fiber photometry, chemogenetic manipulations and behavioral tests, we demonstrated for the first time that the important role and function of GPR17 in the regulation of anxiety-like behaviors, as well as the underlying mechanisms.

2. Methods and materials

2.1. Animals

Male C57BL/6J mice (6−8 weeks) were acquired from the Medical Center of Yangzhou University (Yangzhou, China) and housed in a stable environment with 22 ± 2 °C temperature, 55 ± 5% humidity and a 12-h/12-h light/dark cycle (lights on at 7:00 am) for 7 days before the experiment. Mice freely ate food and drank water. All experiments were carried out in accordance with the U.S. National Institutes of Health Guidelines and approved by the Animal Ethics Committee of China Pharmaceutical University (Nanjing, China).

2.2. Chronic restraint stress (CRS) model

We used the CRS model as previously described[28-31]. Each mouse was individually acclimated in a homecage for 3 days before CRS. Then the mouse was placed into the custom-made tube, in which the mouse was not free to move but could breathe freely for 2 h a day for 14 consecutive days. All tubes were cleaned with water and disinfected with a 75% alcohol solution after each use.

2.3. Behavioral tests

All the mice were habituated to the experimental room 40 min before the test. After each behavioral test, 75% ethanol was used to clean the experimental apparatus. All the tests were performed by a technician blinded to the treatment group and the data were recorded using the video-tracking system (Jiliang, China). All the heatmap plots were performed by ANY-maze (Stoelting, USA).

2.3.1. Open field test (OFT)

Each mouse was placed into the center of an open rectangle field (50 cm × 50 cm × 40 cm) and allowed to explore the apparatus for 6 min freely. The digital video-tracking system recorded the time spent in the center and total distance in OFT.

2.3.2. Elevated plus maze (EPM) test

The apparatus (55 cm height) consisted of two open arms (30 cm × 5 cm, without walls) and two closed arms (30 cm × 5 cm, with 15 cm height walls). Each mouse was put into the center of the apparatus and explored for 6 min. The video-tracking system recorded the time spent in open arms and closed arms, the entries of open arms and closed arms.

2.3.3. Novelty suppressed feeding (NSF) test

Each mouse suffered 24 h of fasting before the test. Then the mouse was placed into one corner of the field (50 cm × 50 cm × 40 cm) and a piece of food pellet was placed in the center of the field. The video-tracking system recorded the time when the mouse ate the pellet firstly and allowed the mouse to explore up to 10 min. The mouse was immediately transformed into the homecage when they initially bit the food. The weight of the consumed food was recorded for 30 min.

2.3.4. Tail suspension test (TST)

Each mouse was suspended from a 50 cm high device by adhesive tape. The test lasted for 6 min and recorded the duration of immobility time.

2.3.5. Forced swim test (FST)

Each mouse was put into a transparent cylinder (20 cm in diameter, 33 cm in height) filling with 20 cm-deep and 22−25 °C temperature water. The test lasted for 6 min and recorded the duration of immobility time.

2.3.6. Sucrose preference test (SPT)

The test consisted of three phases and mice were housed individually during the test. First, the mouse was supplied with two bottles of water for 24 h. Then, the water was replaced with 1% sucrose solution for 24 h. At last, the mouse was supplied with a

bottle of water and a bottle of 1% sucrose solution after the deprivation of water for 24 h, and the locations of the two bottles were changed every 6 h to avoid place preference and the 12-h consumption of each bottle was recorded. SPT was calculated according to Eq. (1):

$$\text{The sucrose preference index} = \text{Sucrose consumption}/(\text{Sucrose} + \text{Water consumption}) \quad (1)$$

2.4. Surgery and stereotaxic injection

Each mouse was anesthetized with 5% isoflurane (RWD Life Science, China) for induction and 2.5% isoflurane for maintenance. Then the mouse was positioned in a stereotaxic frame (Harvard Apparatus, America). Specific viruses at a volume of 200 nL were microinfused into the target regions (50 nL/min) with a microinjection pump (Harvard, USA). The microliter syringe (Gaoge, China) was left at the injection site for 10 min to ensure spreading virus totally after the microinjection. The coordinates of each brain region were as follows: basolateral amygdala (BLA) (AP, −1.45 mm; ML, ±3.20 mm; DV, −4.9 mm), ventral hippocampal CA1 (vCA1) (AP, −3.28 mm; ML, ±3.3 mm; DV, −4.5 mm). AP, ML, DV represented the anterior−posterior, medial−lateral, dorsal−ventral positions relative to the bregma. Details of all Adeno-associated viruses were listed in Supporting Information Table S1.

For specific knockdown of GPR17 in BLA glutamatergic neurons, $AAV_{2/9}$-CaMKIIα-*Gpr17* shRNA-mCherry or the control vector $AAV_{2/9}$-CaMKIIα-NC shRNA-mCherry was bilaterally injected into BLA.

For specific overexpression of GPR17 in BLA glutamatergic neurons, $AAV_{2/9}$-CaMKIIα-*Gpr17*-mCherry or the control vector $AAV_{2/9}$-CaMKIIα-NC-mCherry was bilaterally injected into BLA.

For monosynaptic anterograde tracing, $AAV_{2/9}$-CaMKIIα-mCherry which could spread anterogradely to the downstream regions along the axons was bilaterally injected into BLA.

2.5. Cannula implantation and infusion of drugs

To identify the effects of the GPR17 antagonist on anxiety-like behaviors of CRS mice, the cannulas (27 G, C.C = 5.0 mm; RWD Life Science, China) were implanted bilaterally into BLA. After 3 days, cangrelor (0.5 nmol/per site, 1 nmol/per mouse) (163706-36-3, Aladdin Bio-Chem Technology, China) was injected through the cannulas once a day for 3 consecutive days and continued to be injected once a day 30 min before the behavioral tests.

To identify whether the anxiolytic-like effects of GPR17 antagonist depend on BLA glutaminergic neuronal activity or vCA1 pyramidal neuronal activity, we bilaterally implanted cannulas (27 G, C.C = 5.0 mm; RWD Life Science, China) into BLA to inject cangrelor (0.5 nmol/per site, 1 nmol/per mouse) three weeks after the 200 nL $AAV_{2/9}$-CaMKIIα-hM3Dq-mCherry injecting into BLA or vCA1.

To identify the effects of GPR17 antagonist on glutaminergic neuronal activity and glutamate release in BLA, we bilaterally implanted cannulas (23 G, C.C = 5.0 mm; RWD Life Science, China) into BLA to inject cangrelor (0.5 nmol/per site, 1 nmol/per mouse) and inserted optical fibers (200 μm in diameter, NA 0.37, Inper, China) above the BLA three weeks after the 200 nL $AAV_{2/9}$-CaMKIIα-GCaMP6s or $AAV_{2/9}$-hSyn-iGluSnFR injecting into BLA.

To identify the effects of GPR17 antagonist on pyramidal neuronal activity and glutamate level in vCA1, we bilaterally implanted cannulas (27 G, C.C = 5.0 mm; RWD Life Science, China) into BLA to inject cangrelor (0.5 nmol/per site, 1 nmol/per mouse) and inserted optical fibers (200 μm in diameter, NA 0.37, Inper, China) above the vCA1 three weeks after the 200 nL $AAV_{2/9}$-CaMKIIα-GCaMP6s or $AAV_{2/9}$-hSyn-iGluSnFR injecting into BLA.

2.6. Chemogenetic manipulations

For chemogenetic activation of BLA glutamatergic neurons or vCA1 PyNs, 200 nL $AAV_{2/9}$-CaMKIIα-hM3Dq-mCherry was bilaterally injected into BLA or vCA1 and Clozapine-*N*-oxide (CNO, 2 mg/kg, MedChemExpress, USA) was intraperitoneally injected to activate the glutamatergic neurons.

2.7. Fiber photometry

For fiber photometry, 200 nL $AAV_{2/9}$-CaMKIIα-GCaMP6s or $AAV_{2/9}$-hSyn-iGluSnFR was bilaterally injected into BLA. Three weeks later, ceramic ferrule with optical fiber (200 μm in diameter, NA 0.37, Inper, China) was bilaterally implanted above the BLA or vCA1 and was fastened using denture base materials (Sncdental, China). After implantation for 3 days, fiber photometry was performed to record the calcium signals or glutamate signals during the EPM test using the fiber photometry system (Inper, China).

There were two excitation wavelengths, which were 470 nm excited fluorescence signal and 410 nm as the control signal. The original data were corrected by Inper Data Process software and segmented according to behavioral events within individual trials. The time point of entering the open arm was defined as 0 s and the value of the signal between −5 s and 0 s was set to the baseline. We analyzed area under curve (AUC) and the $\Delta F/F_0$ [Eq. (2)]:

$$\Delta F/F_0\ (\%) = [(F - F_0)/F_0 \times 100] \quad (2)$$

which was performed with heatmaps and average plots by MATLAB.

2.8. Immunofluorescence

Mice were anesthetized and perfused with PBS, followed by 4% paraformaldehyde. Each mouse brain was collected and stored in 4% paraformaldehyde overnight and dehydrated in 30% sucrose for 2 days.

For frozen slices, a freezing microtome (CM1950, Leica, Germany) was used to cut coronal brain slices with a thickness of 25 μm. After blocking in 10% Donkey serum (SL050, Solarbio Life Science, China) and 0.3% Triton X-100 (ST795, Beyotime, China) for 1.5 h at room temperature, the brain slices were incubated with primary antibodies, such as goat anti-GPR17 (1:50, sc-74792, Santa Cruz Biotechnology, USA), mouse anti-CaMKIIα (1:50, sc-13141, Santa Cruz Biotechnology, USA), chicken anti-NeuN (1:500, ABN91, Sigma−Aldrich, USA) and rabbit anti-c-Fos (1:500, 226008, Synaptic Systems, Germany) in 4 °C overnight. On the second day, the slices were washed three 5-min washes in PBS and then incubated for 2 h with Alexa Fluor 594-conjugated secondary antibody and/or Alexa Fluor 488-conjugated secondary antibody (1:500, Yeasen Biotechnology, China)

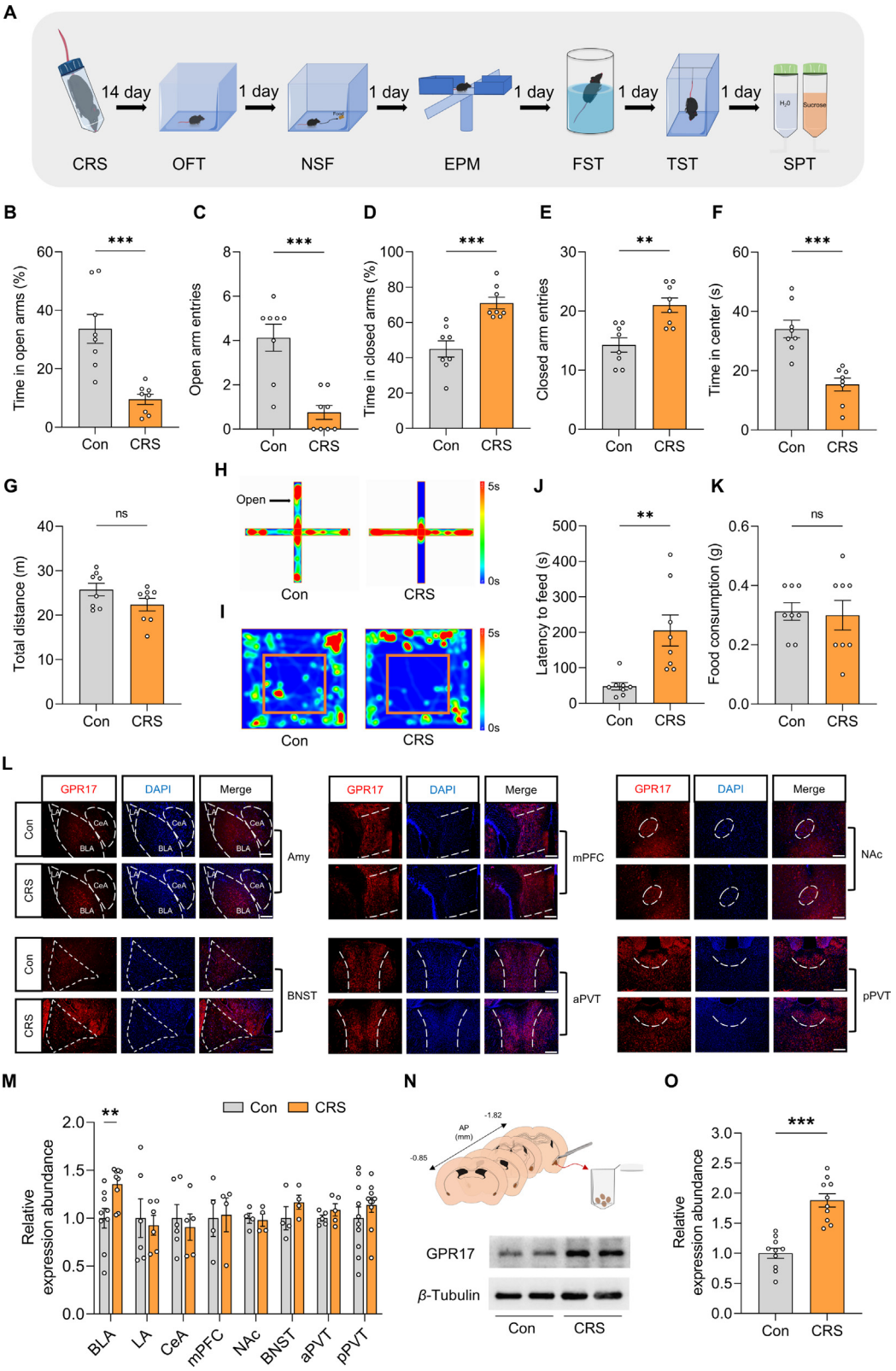

Figure 1 CRS induces anxiety-like behaviors and increases GPR17 expression in BLA. (A) Experimental procedures. Statistical data of time in open arms (B), open arms entries (C), time in closed arms (D) and closed arm entries (E) in EPM test ($n = 8$). Statistical data of time in center (F) and total distance traveled (G) in OFT ($n = 8$). Representative heat-map plots in EPM test (H) and OFT (I). Statistical data of latency to feed (J) and food consumption (K) in NSF test ($n = 8$). (L) Representative images of GPR17 immunofluorescence staining in BLA, LA, CeA, mPFC, NAc, BNST, aPVT and pPVT. Scale bars = 100 μm. (M) Statistical data shows relative expression abundance of GPR17 in different brain regions ($n = 4-10$). (N) Schematic of extracting the BLA for Western blot assays (top) and representative bands of GPR17 expression in BLA (bottom).

in the dark at room temperature. Nuclei were stained by DAPI (C0065, Solarbio Life Science, China).

For paraffin slices, 4 μm coronal sections were prepared by AiFang Biological (China). After warming at 60 °C for 40 min, slices were dewaxed using xylenes for 20 min twice, ethanol for 5 min twice and 75% ethanol for 5 min once, then washed with PBS. For antigen repair, the slices were heated in the microwave oven under the condition of low-power heating for 8 min, keeping warm for 7 min, and medium-low-power heating for 7 min with Tris−EDTA (G1207, Servicebio, China). After naturally cooled, slices were washed three 5-min washes in PBS. Other steps of blocking, primary antibody, secondary antibody and DAPI were the same as those of frozen slices.

Paraffin slices were used to co-stain GPR17 with CaMKIIα and other staining used frozen slices. All immunofluorescent images were obtained by fluorescence microscope (DM 2000, Lecia, Germany). Then, the cell staining was counted using NIH Image J software by an experimenter blinded to the treatment groups.

2.9. Western blot

For isolating different brain regions for Western blot, the extracted brains were sectioned into 1 mm thick coronal slices by a mouse brain matrix and these regions were identified according to the mouse brain atlas under observation of stereomicroscope. According to the weight of the target brain regions, we added lysis buffer (BC 3710, Solarbio Life Science, China) to homogenize total proteins and centrifugated the supernatants at 10,008 × *g* for 8 min at 4 °C to collect the protein. BCA kits (P0012S, Beyotime, China) were used to measure the concentration of the protein. The equal amount of protein was separated by SDS-PAGE for 90 min and transferred onto a PVDF membrane (Merck, Germany). The membranes were blocked by 5% skim milk for 2 h at room temperature and incubated overnight at 4 °C with goat anti-GPR17 (1:500, sc-74792, Santa Cruz, USA) or rabbit anti-β-Tubulin (1:5000, BS 70187, bioworlde, China). After washing three 5-min in TBST, the membranes were incubated with the secondary antibodies (1:5000, HA 1006, Huabio, China) for 2 h. Enhanced chemiluminescence detection reagents and a gel imaging system (Tanon, China) were used to observe the antibody-reactive bands.

2.10. In vitro electrophysiology recordings

Mice were anesthetized with isoflurane and perfused with ice-cold sucrose-based ACSF containing (in mmol/L): 40 NaCl, 4.5 KCl, 1.25 NaH_2PO_4, 25 $NaHCO_3$, 148.5 sucrose, 10 glucose, 1 ascorbic acid, 3 Na Pyruvate, 3 Myo Inositol, 0.5 $CaCl_2$ and 7 $MgSO_4$. 300 μm coronal slices containing BLA or vCA1 were sectioned in ice-cold sucrose-based artificial cerebrospinal fluid using a VT1200S vibratome (Leica, Germany) and then recovered in warm artificial cerebrospinal fluid containing (in mmol/L): 125 NaCl, 4.5 KCl, 1.25 NaH_2PO_4, 25 $NaHCO_3$, 15 sucrose, 15 glucose, 2.5 $CaCl_2$ and 1.3 $MgSO_4$ for 30 min at 35 °C. Before recording, slices were allowed to cool in room temperature for at least 30 min. All solutions were continually saturated with 95% O_2 and 5% CO_2 before and during use.

For action potentials and rheobase recordings, $AAV_{2/9}$-CaMKIIα-mCherry was injected into BLA and whole-cell current-clamp mode was applied using pipettes (4−6 MΩ, Sutter Instrument, USA) filled with an internal solution containing (in mmol/L): 127 K-gluconate, 13 KCl, 4 Mg3-ATP, 0.3 Na3-GTP, 0.3 EGTA, 10 HEPES and 10 Na-phosphocreatine (pH 7.25, 290 mOsm). Currents ranging from −20 to 160 pA were injected into BLA glutamatergic neurons with a step of 20 pA to evoke action potentials. Rheobase was defined as the value of current amplitude at which an action potential was first evoked. Cangrelor (100 nmol/L) was applied to inhibit GPR17.

For opto-evoked excitatory postsynaptic currents (oEPSCs) recordings, $AAV_{2/9}$-CaMKIIα-ChR2-mCherry was injected into BLA to optogenetic activate BLA-vCA1 circuit, $AAV_{2/9}$-CaMKIIα-EGFP was injected into vCA1 to label PyNs, and then whole-cell voltage-clamp mode was applied with pipettes filled with an internal solution containing (in mmol/L): 132.5 Cs-gluconate, 17.5 CsCl, 2 $MgCl_2$, 0.5 EGTA, 10 HEPES, 4 ATP, 5 QX-314 (pH 7.25, 290 mOsm). vCA1 PyNs were visualized by fluorescence microscopy (Olympus, Japan) and held at −70 mV during recording. A 10 ms 470 nm light was delivered to BLA glutamatergic terminals by an LED illuminant (Mightex, Canada) under the control of Digidata 1550B (Axon, USA) to arouse EPSCs. All traces were recorded by Clampex 11.1 (Molecular Devices, USA) using MultiClamp 700B Commander (Axon, USA) and analyzed by Clampfit 11.1 (Molecular Devices, USA).

2.11. Statistical analysis

GraphPad Prism v9.3.1 was used to analyze all data. The two-tailed unpaired Student's *t* tests for two groups, one-way analysis of variance (ANOVA) or two-way ANOVA with Bonferroni, Tukey and LSD *post hoc* comparison test for multiple comparisons were used. All experimental data were represented as mean ± standard error of the mean (SEM). Significance levels were indicated as *ns* $P > 0.05$, $^*P < 0.05$, $^{**}P < 0.01$, $^{***}P < 0.001$.

3. Results

3.1. CRS induces anxiety-like behaviors and increases GPR17 expression in BLA

Firstly, we used CRS to induce the anxiety-like behaviors of mice. As expected, we found that compared with the control mice, CRS group mice exhibited significant anxiety-like behaviors in EPM, OFT and NSF tests (Fig. 1A−K). Meanwhile, no significant difference in depression-like behaviors was evidenced by the unchanged immobility time in FST and TST and the sucrose preference in SPT between the two groups (Supporting Information Fig. S1A−S1C). Moreover, the body weight of CRS group mice continuously decreased from day 3 to day 14 (Fig. S1D). These results suggest that CRS successfully induced anxiety-like behaviors in mice.

(O) Quantitative analysis of GPR17 expression in BLA ($n = 10$). All data are expressed as the mean ± SEM. ns $P > 0.05$; $^{**}P < 0.01$; $^{***}P < 0.001$. Con, control; CRS, chronic restraint stress; EPM, elevated plus maze; OFT, open field test; NSF, novelty suppressed feeding; FST, forced swim test; TST, tail suspension test; SPT, sucrose preference test; BLA, basolateral amygdala; LA, lateral amygdala; CeA, central amygdala; mPFC, medial prefrontal cortex; NAc, nucleus accumbens; BNST, bed nucleus of the stria terminalis; aPVT, anterior paraventricular thalamic nucleus; pPVT, posterior paraventricular thalamic nucleus.

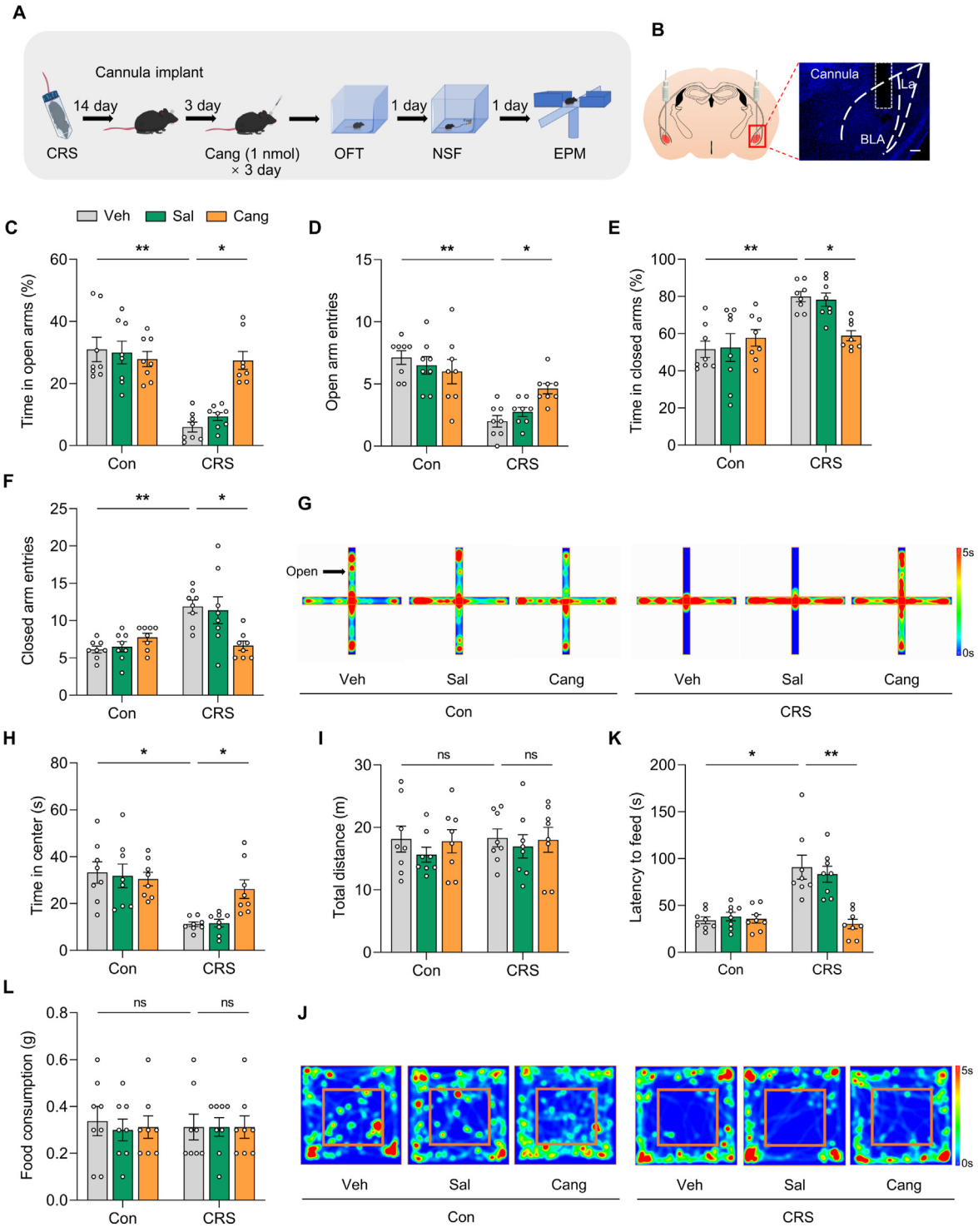

Figure 2 GPR17 antagonist cangrelor ameliorates CRS-induced anxiety-like behaviors in mice. (A) Experimental procedures. (B) Representative images of cannula site in BLA. Statistical data of time in open arms (C), open arm entries (D), time in closed arms (E), closed arm entries (F) and heat-map plots (G) in EPM test ($n = 8$). Statistical data of time in center (H), total distance (I) and heat-map plots (J) in OFT ($n = 8$). Statistical data of latency to feed (K) and food consumption (L) in NSF test ($n = 8$). All data are expressed as the mean ± SEM. ns $P > 0.05$; *$P < 0.05$; **$P < 0.01$. Veh, vehicle; Sal, saline; Cang, cangrelor.

We then detected the expression of GPR17 in different brain regions related to anxiety after CRS. Immunofluorescence showed that GPR17 expression was significantly increased only in BLA after CRS exposure (Fig. 1L and M). Consistently, compared with the control mice, the protein expression of GPR17 was also dramatically elevated only in BLA after CRS (Fig. 1N, O and Fig. S1E and S1F). Taken together, these data indicate that GPR17 in BLA might be involved in anxiety-like behaviors.

3.2. GPR17 antagonist cangrelor ameliorates CRS-induced anxiety-like behaviors in mice

We then wondered whether inhibiting GPR17 in BLA ameliorates the anxiety-like behaviors in CRS mice. After CRS, cannulas were bilaterally implanted in BLA. Then, cangrelor was injected by cannulas for 3 consecutive days. Different behavioral tests were performed to detect anxiety-like behaviors and cangrelor continued to be injected once a day 30 min before each behavioral test (Fig. 2A and B). The results showed that cangrelor significantly increased the time spent in open arms and entries of open arms, while significantly decreased the time spent in closed arms and entries of closed arms of CRS mice in the EPM test (Fig. 2C−G). In addition, cangrelor significantly increased time in the center and displayed no significant difference traveled in the total distance of CRS mice in OFT (Fig. 2H−J). Cangrelor significantly reduced the latency to feed and had no influence on the food consumption of CRS mice in the NSF test (Fig. 2K and L). These data suggest that pharmacological inhibition of GPR17 in BLA ameliorates CRS-induced anxiety-like behaviors and cangrelor has a prominently anxiolytic effect in mice.

3.3. CRS-induced anxiety-like behaviors are associated with upregulation of GPR17 in BLA glutamatergic neurons

To determine which cell type of GPR17 takes part in anxiety-like behaviors, we firstly detected the colocation of GPR17 with neuron marker (NeuN) in BLA. Interestingly, we found that about 96.67% of GPR17-positive ($GPR17^+$) cells were labeled with NeuN in BLA of naïve mice (Fig. 3A and B). Furthermore, we found that approximately 91.65% and 92.57% of $GPR17^+$ cells co-expressed with glutamatergic excitatory neuronal marker calcium/calmodulin-dependent protein kinase II α (CaMKIIα) in control and CRS group mice, respectively (Fig. 3C and D). More importantly, the number of $GPR17^+$ and CaMKIIα-positive ($CaMKII\alpha^+$) colocalized cells was significantly increased in BLA of CRS mice compared to control mice (Fig. 3C and E). These findings suggest that GPR17 is mainly expressed in BLA gluta-

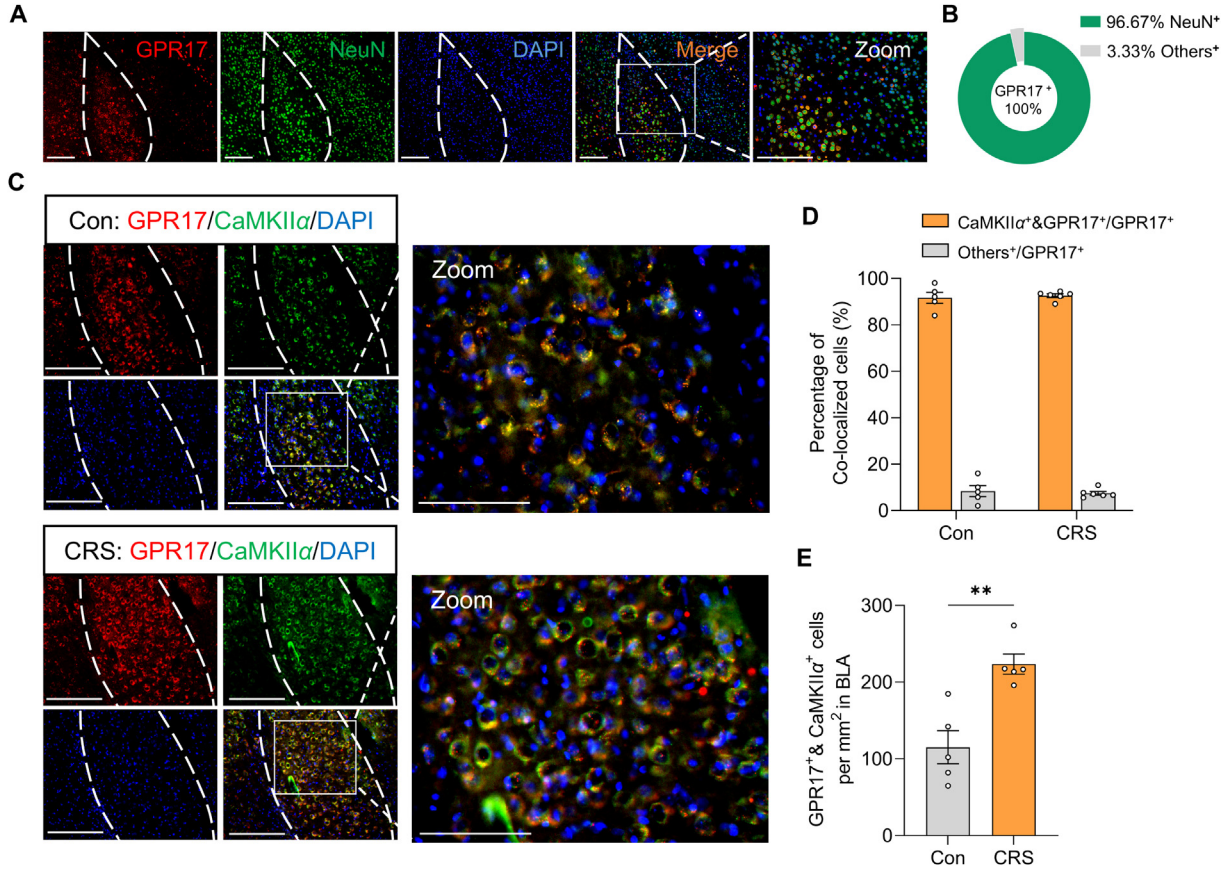

Figure 3 CRS-induced anxiety-like behaviors are associated with upregulation of GPR17 in BLA glutamatergic neurons. CRS was used to induce anxiety-like behaviors and then brains were collected to perform immunofluorescence. (A) Representative images for colocalization of $NeuN^+$ and $GPR17^+$ cells in BLA. Scale bars = 100 μm. (B) Graph shows the percentage of $NeuN^+$ and $GPR17^+$ colocalized cells in total $GPR17^+$ cells in BLA ($n = 8$). (C) Representative images for colocalization of $CaMKII\alpha^+$ and $GPR17^+$ cells in BLA. Scale bars = 100 μm. (D) Graph shows the percentage of $CaMKII\alpha^+$ and $GPR17^+$ colocalized cells or other cells in total $GPR17^+$ cells in BLA ($n = 5$−6). (E) Graph shows the number of $GPR17^+$ and $CaMKII\alpha^+$ colocalized cells in BLA ($n = 5$). All data are expressed as the mean ± SEM. $^{**}P < 0.01$.

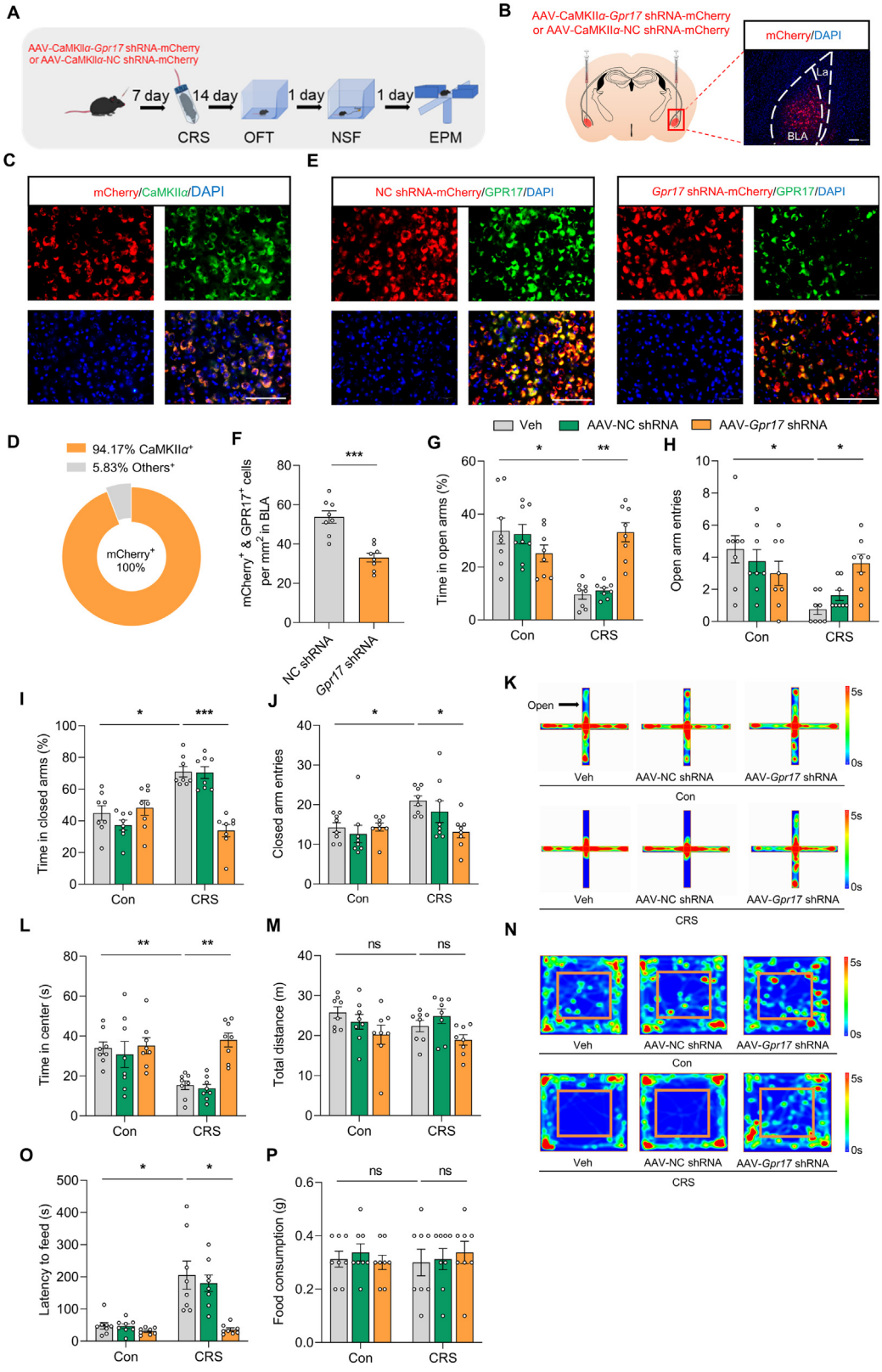

Figure 4 Downregulation of GPR17 in BLA glutamatergic neurons alleviates anxiety-like behaviors in mice. (A) Experimental procedures. (B) Schematic and representative images of viral injection site and expression in BLA. Scale bar = 100 μm. (C) Representative images for colocalization of mCherry$^+$ and CaMKIIα^+ cells in BLA. (D) The immunofluorescence graph shows about 94.17% CaMKIIα^+ cells colocalized with the mCherry $^+$ cells (n = 5). Scale bar = 100 μm. (E) Representative images for colocalization of mCherry$^+$ (red) and GPR17$^+$ (green) cells in BLA. (F) Statistical data of the number of mCherry$^+$ and GPR17$^+$ colocalized cells in BLA (n = 8). Statistical data of time in open arms (G),

matergic neurons, which might be involved in the pathogenesis of CRS-induced anxiety-like behaviors.

3.4. Downregulation of GPR17 in BLA glutamatergic neurons alleviates anxiety-like behaviors in mice

In order to identify the role of GPR17 in BLA glutamatergic neurons in CRS mice, we generated an adeno-associated virus (AAV) vector carrying *Gpr17*-specific short hairpin RNA (shRNA) and red fluorescent protein driven by glutamatergic neuronal promoter (AAV-CaMKIIα-*Gpr17* shRNA-mCherry), which was bilaterally infused into BLA. 7 days after the AAV injection, CRS was applied to induce anxiety-like behaviors and then various behavioral tests were performed (Fig. 4A and B). Firstly, we verified that about 94.17% CaMKIIα neurons colocalized with mCherry in BLA after injection of AAV-CaMKIIα-*Gpr17* shRNA-mCherry (Fig. 4C and D), demonstrating the AAV is specific to glutamatergic neurons. Then, we found the number of mCherry$^+$ and GPR17$^+$ colocalized cells and the protein levels of GPR17 in BLA were significantly decreased in the mice infused with AAV-CaMKIIα-*Gpr17* shRNA-mCherry, confirming GPR17 is downregulated in BLA glutamatergic neurons (Fig. 4E and F and Supporting Information Fig. S2A and S2B). More importantly, we found GPR17 knockdown in BLA glutamatergic neurons reversed the decrease of time in open arms and entries of open arms and the increase of time in closed arms and entries of closed arms in the EPM test (Fig. 4G−K), which was induced by CRS. Moreover, GPR17 knockdown significantly increased time in the center in OFT (Fig. 4L and N) and decreased the latency to feed in the NSF test (Fig. 4O) in CRS mice. However, GPR17 knockdown did not alter the total distance traveled in the OFT (Fig. 4M) and total food consumption in the NSF test (Fig. 4P) in CRS mice. To sum up, these results demonstrate that specifical knockdown of GPR17 in BLA glutamatergic neurons alleviates CRS-induced anxiety-like behaviors.

3.5. Upregulation of GPR17 in BLA glutamatergic neurons increases susceptibility to anxiety-like behaviors in mice

To further detect the role of GPR17 in BLA glutamatergic neurons, we infused the AAV vector carrying *Gpr17* with mCherry driven by glutamatergic neuronal promoter (AAV-CaMKIIα-*Gpr17*-mCherry) into the bilateral BLA of naïve mice (Fig. 5A and B). Firstly, we verified that about 92.13% CaMKIIα neurons colocalized with mCherry in BLA after injection of AAV-CaMKIIα-*Gpr17*-mCherry (Fig. 5C and D), demonstrating the AAV is specific to glutamatergic neurons. Then, we found the number of mCherry$^+$ and GPR17$^+$ colocalized cells and the protein levels of GPR17 in BLA were significantly increased in the mice infused with AAV-CaMKIIα-*Gpr17*-mCherry, confirming GPR17 is upregulated in BLA glutamatergic neurons (Fig. 5E and F and Supporting Information Fig. S3M, S3N). Three weeks after the AAV injection, various behavioral tests were performed (Fig. S3A). We found that GPR17 overexpression only significantly decreased the time in open arms, while there was no significant change in other indicators in the EPM test of naïve mice (Fig. S3B−S3E). In addition, GPR17 overexpression significantly decreased time in the center in OFT and increased the latency to feed in NSF test in naïve mice (Fig. S3F−S3I). However, we found that GPR17 overexpression combined with exposure to sub-CRS (three-day CRS) exhibited distinct anxiety-like behaviors in all indicators in EPM, OFT and NSF tests (Fig. 5G−P), and had no significant difference in depression-like behaviors in TST, FST and SPT (Fig. S3J−S3L). Together, these data reveal that overexpression of GPR17 in BLA glutamatergic neurons increases the susceptibility to anxiety-like behaviors in naïve mice.

3.6. BLA glutamatergic neuronal activity is required for anxiolytic-like effects of GPR17 antagonist

We hypothesized that the activity of BLA glutamatergic neurons is critical to the anxiolytic-like effects of the GPR17 antagonist. To address this question, we first used *in vitro* electrophysiology recordings to detect the excitability of BLA glutamatergic neurons. The AAV-CaMKIIα-mCherry was injected into BLA to label glutamatergic neurons, action potentials and rheobase of glutamatergic neurons were recorded from BLA brain slices (Fig. 6A). We found that the firing rate of BLA glutamatergic neurons was significantly increased and the rheobase was dramatically decreased in CRS brain slices compared to the control brain slices (Fig. 6B−D), suggesting that BLA glutamatergic neurons were activated after CRS. However, the presence of GPR17 antagonist cangrelor reversed the changes (Fig. 6B−D).

Then, we used chemogenetic manipulation and *in vivo* fiber photometry to keep track of the excitability of BLA glutamatergic neurons in the EPM test (Fig. 6E−M). AAV-CaMKIIα-hM3Dq-mCherry and AAV-CaMKIIα-GCaMP6s were injected into BLA, 7 days later, CRS was performed and cangrelor was injected into BLA after intraperitoneally injecting CNO for 3 consecutive days. During EPM test, *in vivo* fiber photometry was applied. We found that the calcium signals of glutamatergic neurons in cangrelor-treated mice were significantly decreased compared to the CRS mice when the mice entered the open arms in EPM test, and these were reversed by chemogenetic activation of BLA glutamatergic neurons (Fig. 6H−J). Furthermore, we used iGluSnFR to record the glutamate release in BLA. Similarly, we found that the fluorescence signals depicted a significant decrease in cangrelor-treated mice when the mice entered the open arms in EPM test, and these were reversed by chemogenetic activation of BLA glutamatergic neurons in CRS mice (Fig. 6K−M).

Additionally, to further confirm the results, the number of c-Fos$^+$ cells in BLA was stained after behavioral tests. we found the c-Fos$^+$ cells were significantly increased in CRS mice, and these were reversed by cangrelor (Fig. 6N and O). And the increased c-Fos$^+$ cells were mainly glutamatergic neurons in BLA (Fig. 6P and Q). These data suggest that BLA glutamatergic neuronal activity was increased not only under basal conditions after CRS, but also during behavioral tests when mice entered the open arms in EPM test and after behavioral tests. Moreover, the GPR17 antagonist cangrelor reversed these changes.

To investigate whether the activity of BLA glutamatergic neurons would be sufficient for anxiolytic-like effects of

open arm entries (H), time in closed arms (I), closed arm entries (J) and heat-map plots (K) in EPM test ($n = 8$). Statistical data of time in the center (L), total distance traveled (M) and heat-map plots (N) in OFT ($n = 8$). Statistical data of latency to feed (O) and food consumption (P) in NSF test ($n = 8$). All data are expressed as the mean ± SEM. ns $P > 0.05$; *$P < 0.05$; **$P < 0.01$; ***$P < 0.001$.

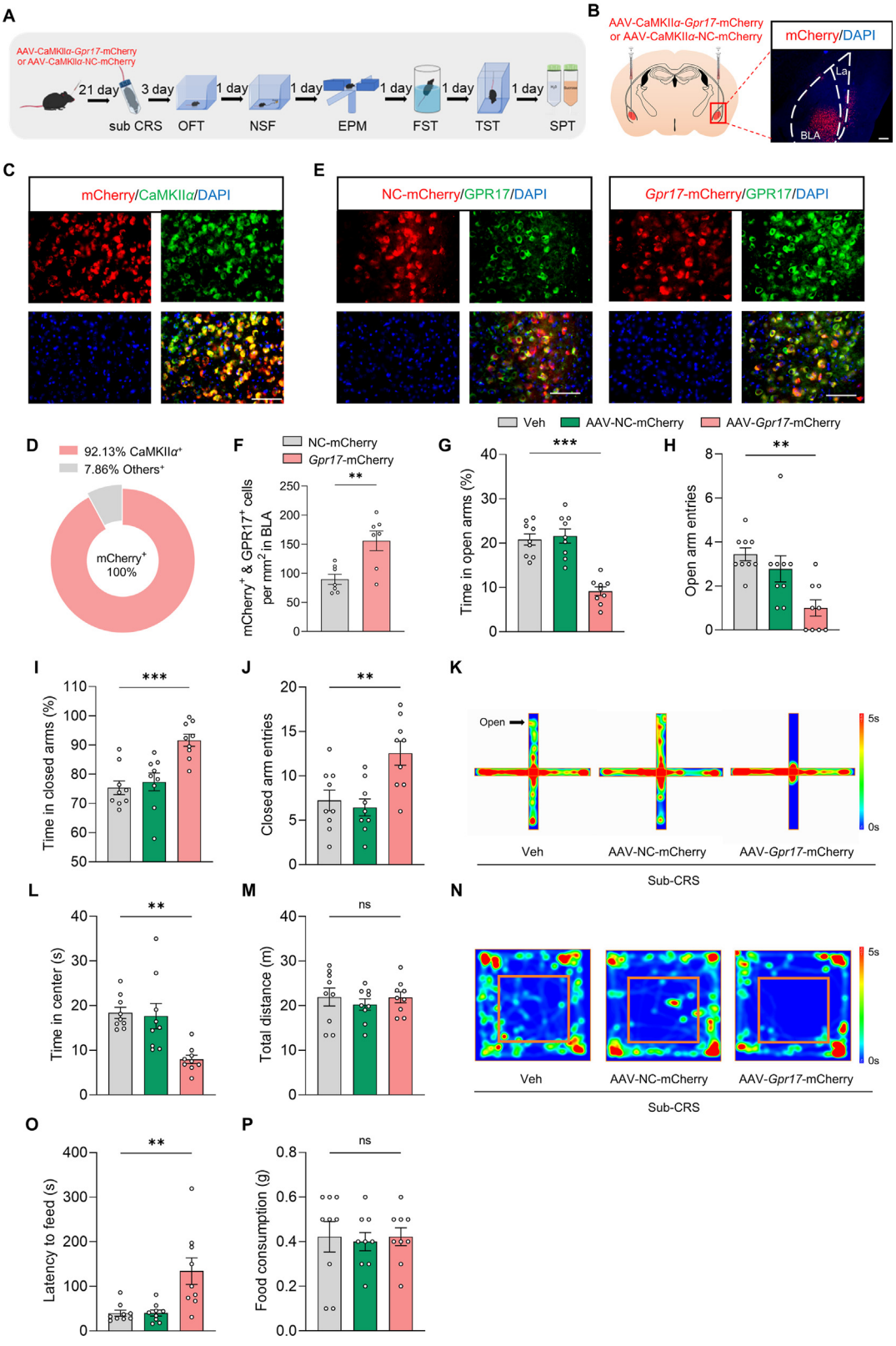

Figure 5 Upregulation of GPR17 in BLA glutamatergic neurons increases susceptibility to anxiety-like behaviors in mice. (A) Experimental procedures. (B) Schematic and representative images of viral injection site and expression in BLA. Scale bar = 100 μm. (C) Representative images for colocalization of mCherry$^+$ and CaMKIIα^+ cells in BLA. (D) The immunofluorescence graph shows about 92.13% CaMKIIα^+ cells colocalized with mCherry $^+$ cells (n = 4). Scale bar = 100 μm. (E) Representative images for colocalization of mCherry$^+$ and GPR17$^+$ cells in BLA. (F) Statistical data of the number of mCherry$^+$ and GPR17$^+$ colocalized cells in BLA (n = 7). Statistical data of time in open arms (G), open arm entries (H), time in closed arms (I), closed arm entries (J) and heat-map plots (K) in EPM test (n = 9). Statistical data of time in center

cangrelor. Mice were infused with AAV-CaMKIIα-hM3Dq-mCherry into BLA. The cannulas were bilaterally implanted into BLA after CRS. CNO was intraperitoneally injected 30 min before injecting cangrelor into BLA for 3 consecutive days. Then, the anxiety-like behaviors were measured by different behavioral tests (Fig. 7A and B). The efficiency of AAV-CaMKIIα-hM3Dq-mCherry was verified by immunofluorescence (Supporting Information Fig. S4A−S4D). Compared to the CRS group, cangrelor group mice displayed anxiolytic-like behaviors in EPM, OFT and NSF tests (Fig. 7C−L). Whereas, chemogenetic activation of BLA glutamatergic neurons reversed the anxiolytic-like effects of cangrelor in CRS mice (Fig. 7C−L). Taken together, these data reveal that BLA glutamatergic neuronal activity is required for anxiolytic-like effects of the GPR17 antagonist.

3.7. GPR17 modulates anxiety-like behaviors via BLA to vCA1 glutamatergic projection

The role of BLA in regulating anxiety-like behaviors is probably related to other brain regions. Therefore, we injected AAV-CaMKIIα-mCherry into BLA and found that BLA glutamatergic neurons projected to infralimbic cortex, prelimbic cortex, bed nucleus of stria terminalis, dorsal and ventral hippocampus and lateral septal nucleus (Fig. 8A−C, Supporting Information Fig. S5A). However, only the number of c-Fos$^+$ cells in vCA1 was remarkably increased in CRS mice, without obvious alteration in other regions, and these were reversed by cangrelor (Fig. 8D, E and Fig. S5B and S5C). Moreover, we found the c-Fos$^+$ cells were PyNs and the number of c-Fos$^+$ and PyNs co-labeled cells in vCA1 was significantly decreased after injection cangrelor into BLA in CRS mice, suggesting vCA1 is a major downstream of BLA and might involve in anxiety-like behaviors regulated by GPR17 (Fig. 8F and G). To determine whether glutamatergic transmission was involved in the modulation of GPR17 in anxiety-like behaviors *via* the BLA-vCA1 circuit, we tested the effects of cangrelor on oEPSCs of the BLA-vCA1 circuit. AAV-CaMKIIα-ChR2-mCherry was injected into BLA for optogenetic manipulation of the BLA-vCA1 circuit and AAV-CaMKIIα-EGFP was injected in vCA1 to label PyNs. After CRS, cangrelor was injected into BLA by cannulas for 3 consecutive days and oEPSCs were recorded in vCA1 PyNs after blue light stimulation which could optogenetically activate the BLA-vCA1 circuit (Fig. 8H). We found that blue light stimulation (blue lines) evoked inward currents in vCA1 PyNs receiving BLA glutamatergic neurons projection and increased amplitude of oEPSCs in CRS mice (Fig. 8I and J). While, cangrelor remarkably decreased the amplitude of oEPSCs in vCA1 PyNs of CRS mice (Fig. 8I and J), suggesting the BLA-vCA1 circuit is glutamatergic transmission and is regulated by GPR17. To further prove this finding, we infused AAV-CaMKIIα-GCaMP6s or AAV-hSyn-iGluSnFR into BLA and injected cangrelor into BLA for 3 consecutive days. We found that the neuronal activity and glutamate release were significantly increased in vCA1 PyNs of CRS mice, and these were reversed by cangrelor (Fig. 8K−P). These data reveal that GPR17 modulates BLA to vCA1 glutamatergic projection in CRS mice.

To clarify the role of BLA to vCA1 glutamatergic projection in GPR17-mediated anxiety-like behaviors, AAV-CaMKIIα-hM3Dq-mCherry was bilaterally infused into vCA1. After CRS, the mice were bilaterally implanted cannulas into BLA. CNO was intraperitoneally injected 30 min before cangrelor injected into BLA for 3 consecutive days. Then, the anxiety-like behaviors were measured by different behavioral tests (Fig. 9A and B). We found that chemogenetic activation of vCA1 PyNs reversed the anxiolytic-like effects of cangrelor in EPM, OFT and NSF tests (Fig. 9C−L). Collectively, these data confirm that GPR17 modulates anxiety-like behaviors *via* BLA to vCA1 glutamatergic projection.

4. Discussion

In this study, we found for the first time that the expression of GPR17 was increased in BLA glutamatergic neurons of CRS-induced anxiety-like mice. More importantly, we confirmed that downregulation of GPR17 in BLA glutamatergic neurons alleviated anxiety-like behaviors by inhibiting BLA glutamatergic neuronal excitability, reducing the release of neurotransmitter glutamate, and weakening the neural projection from BLA to vCA1.

Anxiety disorders are classified as circuit disorders involving numerous brain regions, such as medial prefrontal cortex, nucleus accumbens, bed nucleus of the stria terminalis, paraventricular nucleus of the thalamus, amygdala, etc.[32-34]. Our results showed that CRS increased GPR17 expression in amygdala, especially BLA, and pharmacological inhibition of GPR17 in BLA ameliorates CRS-induced anxiety-like behaviors. The amygdala, as one of the key structures of the limbic system, includes the basolateral, central, and lateral subregions. Many researches have shown that the amygdala has an important role in the regulation of emotional behaviors, such as anxiety, fear learning, and depression[35-37]. Different subregions of the amygdala have different cell types. The BLA contains about 85% glutamatergic excitatory neurons and 15% inhibitory interneurons[38-40]. In this study, we found that GPR17 was mainly located in BLA glutamatergic neurons. What's more, specific knockdown of GPR17 in BLA glutamatergic neurons by delivery of AAV-CaMKIIα-*Gpr17* shRNA-mCherry alleviated anxiety-like behaviors and upregulation of GPR17 in BLA glutamatergic neurons by delivery of AAV-CaMKIIα-*Gpr17*-mCherry increased susceptibility to anxiety-like behaviors in mice. These suggest GPR17 is involved in CRS-induced anxiety-like behaviors, and BLA glutamatergic excitatory neurons participate in GPR17-regulated anxiety-like behaviors.

A large number of studies have implicated the glutamatergic system is an important target for developing and treating anxiety disorders. The increased glutamatergic neuronal activity has been proven to enhance anxiety-like behaviors[41-43]. In particular, many studies have reported the glutamatergic neurons in amygdala take part in anxiety-like behaviors and inhibition of the activity of BLA glutamatergic neurons improves anxiety-like behaviors[44-47]. In this study, we found that BLA glutamatergic neuronal activity was significantly increased not only under basal conditions after CRS, but also during behavioral tests when

(L), total distance (M) and heat-map plots (N) in OFT ($n = 9$). Statistical data of latency to feed (O) and food consumption (P) in NSF test ($n = 9$). All data are expressed as the mean ± SEM. ns $P > 0.05$; $^{**}P < 0.01$; $^{***}P < 0.001$.

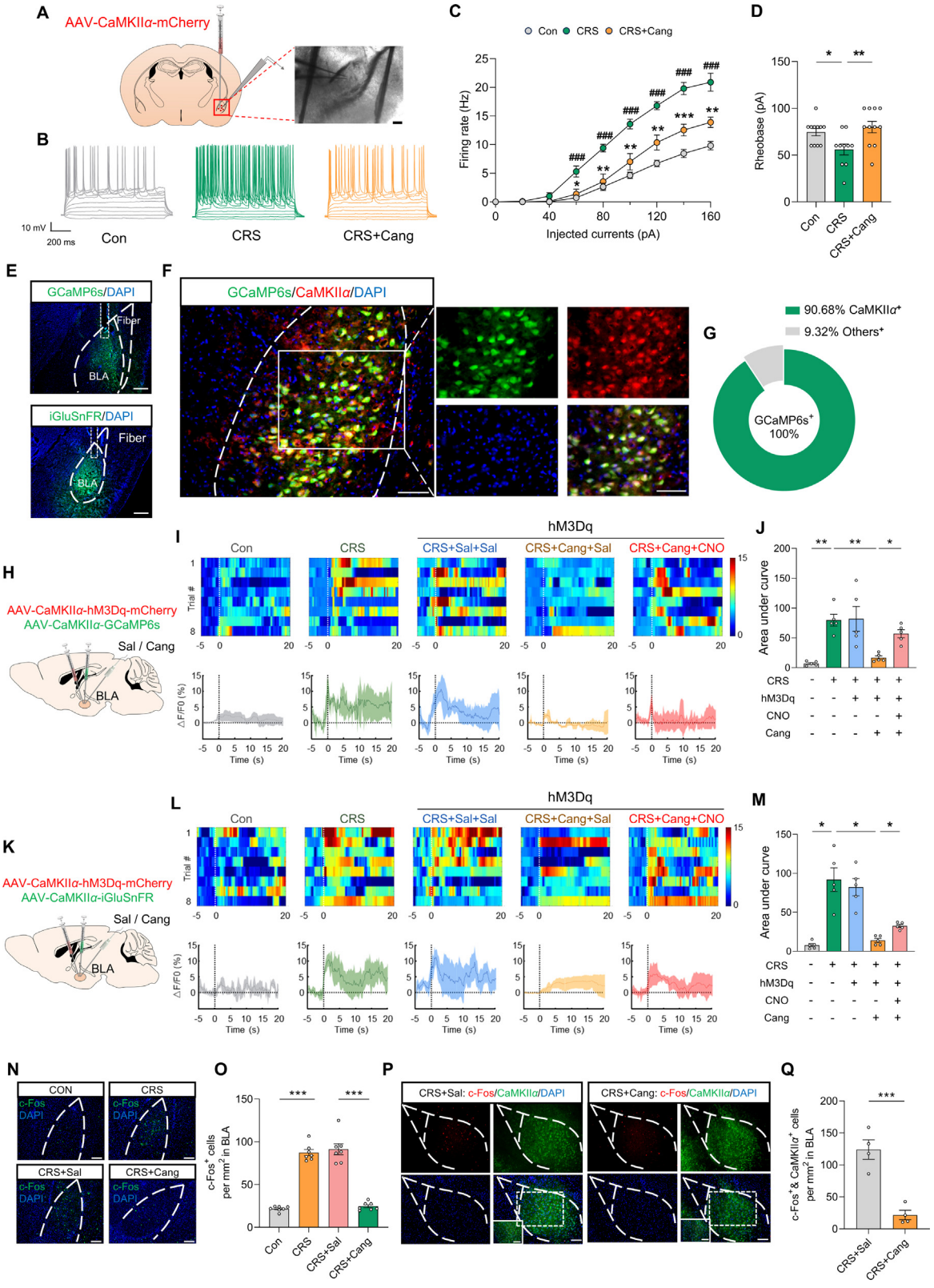

Figure 6 BLA glutamatergic neuron activity and glutamate release are influenced by cangrelor in CRS mice. (A) Schematic of viral injection and whole-cell patch-clamp recording in BLA (left) and representative image of location of electrode (right). Scale bar = 100 μm. (B) Representative traces of action potentials of BLA glutamatergic neurons in brain slices. (C) The firing rate of action potentials evoked by depolarizing current pulses of 0−160 pA (n = 10−11 glutamatergic neurons from 5 mice). $^{\#\#\#}P < 0.001$ Con *vs.* CRS; $^{*}P < 0.05$, $^{**}P < 0.01$, $^{***}P < 0.001$ CRS *vs.* CRS + Cang. (D) Statistical data of rheobase of BLA glutamatergic neurons (n = 10−11 glutamatergic neurons from 5 mice). (E) Representative images of viral injection site and cannula site in BLA. Scale bar = 100 μm. (F) Representative images for colocalization of GCaMP6s^{+} and CaMKIIα^{+} cells in BLA. Scale bar = 100 μm. (G) The immunofluorescence showes about 90.68% GCaMP6s^{+} cells colocalized with CaMKIIα^{+} cells (n = 5). (H) Schematic of viral injection, cannula implantation to inject cangrelor or saline and record Ca^{2+}

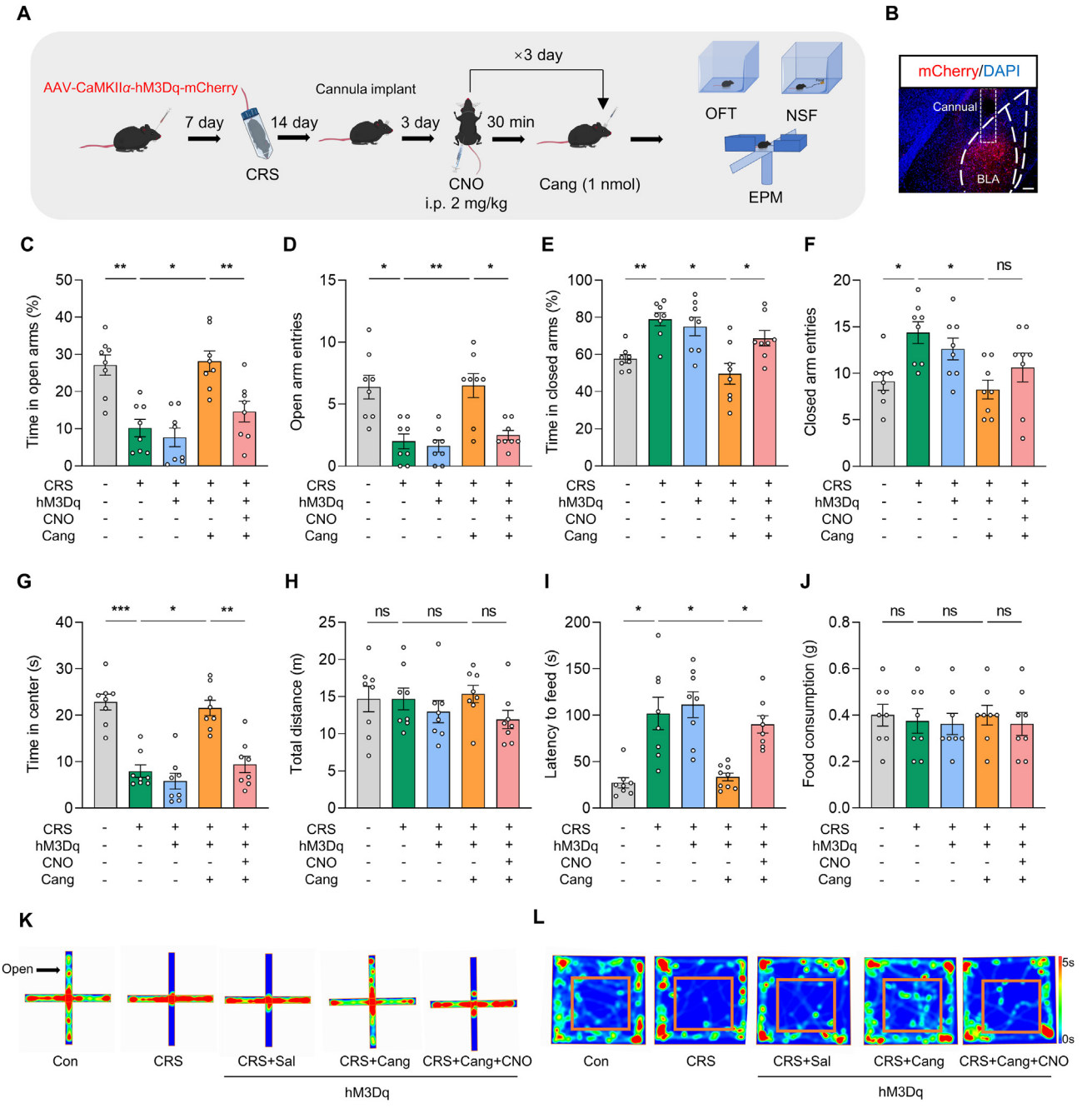

Figure 7 Chemogenetic activation of BLA glutamatergic neurons reverses the anxiolytic-like effects of cangrelor in CRS mice. (A) Experimental procedures. (B) Representative image of viral injection site and cannula site in BLA. Scale bar = 100 μm. Statistic data of time in open arms (C), open arm entries (D), time in closed arms (E) and closed arm entries (F) in EPM test ($n = 8$). Statistical data of time in center (G) and total distance (H) in OFT ($n = 8$). Statistical data of latency to feed (I) and food consumption (J) in NSF test ($n = 8$). Heat-map plot in EPM test (K) and OFT (L). All data are expressed as the mean ± SEM. ns $P > 0.05$; *$P < 0.05$; **$P < 0.01$; ***$P < 0.001$.

signals in BLA. (I) Representative heatmap-plot and averaged traces of normalized Ca^{2+} fluorescence ($\Delta F/F$) ± SEM (shades) in BLA glutamatergic neurons. Time 0 is defined as the moment the mouse entered open arms in EPM test. (J) Statistical data of area under curve in BLA glutamatergic neurons ($n = 5$). (K) Schematic of viral injection, cannula implantation to inject cangrelor or saline and record glutamate signals in BLA. (L) Representative heatmap-plot and averaged traces of normalized glutamate dynamics ($\Delta F/F$) ± SEM (shades) in BLA neurons. Time 0 is defined as the moment the mouse entered open arms in EPM test. (M) Statistical data of area under curve in BLA neurons ($n = 5$). (N) Representative images for c-Fos^+ cells in BLA. Scale bar = 100 μm. (O) Graph shows the number of c-Fos^+ cells in BLA ($n = 7$). (P) Representative images for colocalization of c-Fos^+ and CaMKIIα^+ cells in BLA. Scale bar = 100 μm. (Q) Graph showing the number of c-Fos^+ and CaMKIIα^+ colocalized cells in BLA ($n = 4$). All data are expressed as the mean ± SEM. *$P < 0.05$; **$P < 0.01$; ***$P < 0.001$.

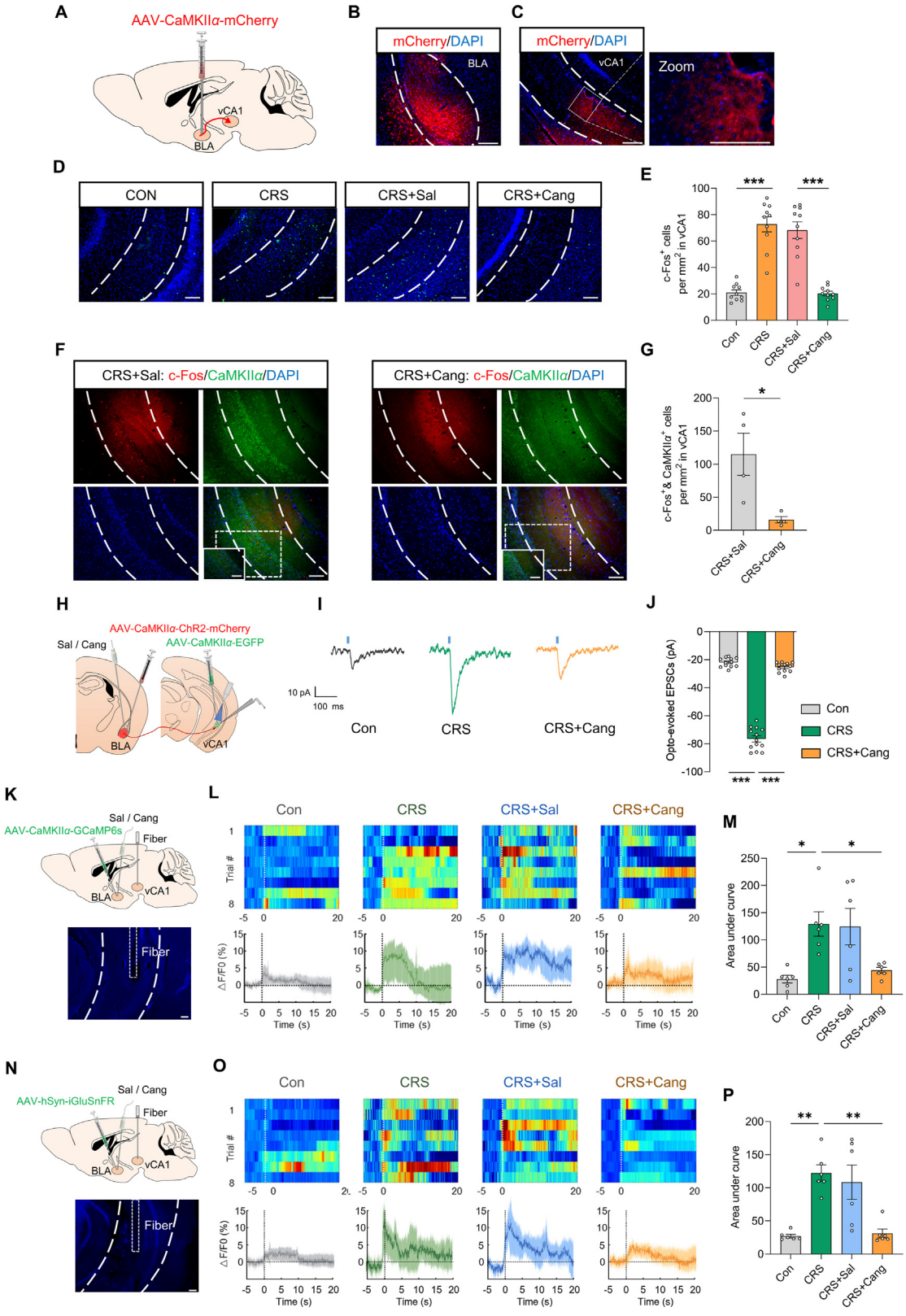

Figure 8 GPR17 modulates BLA to vCA1 glutamatergic projection. (A) Schematic diagram of virus injection. (B) Representative image of the viral injection site. Scale bar = 100 μm. (C) Representative images of axon terminals expressing mCherry in vCA1 originating from BLA glutamatergic neurons. Scale bar = 100 μm. (D) Representative images for c-Fos$^+$ cells in vCA1. Scale bar = 100 μm. (E) Graph shows the number of c-Fos$^+$ cells in vCA1 (n = 10). (F) Representative images for colocalization of c-Fos$^+$ and CaMKIIα^+ cells in vCA1. Scale bar = 100 μm. (G) Graph shows the number of c-Fos$^+$ and CaMKIIα^+ colocalized cells in vCA1 (n = 4). (H) Schematic of *in vitro* electrophysiology recordings. (I) Representative tracks of oEPSCs in vCA1. (J) Statistical data of oEPSCs in vCA1 (n = 12−13 PyNs from 5 mice). (K)

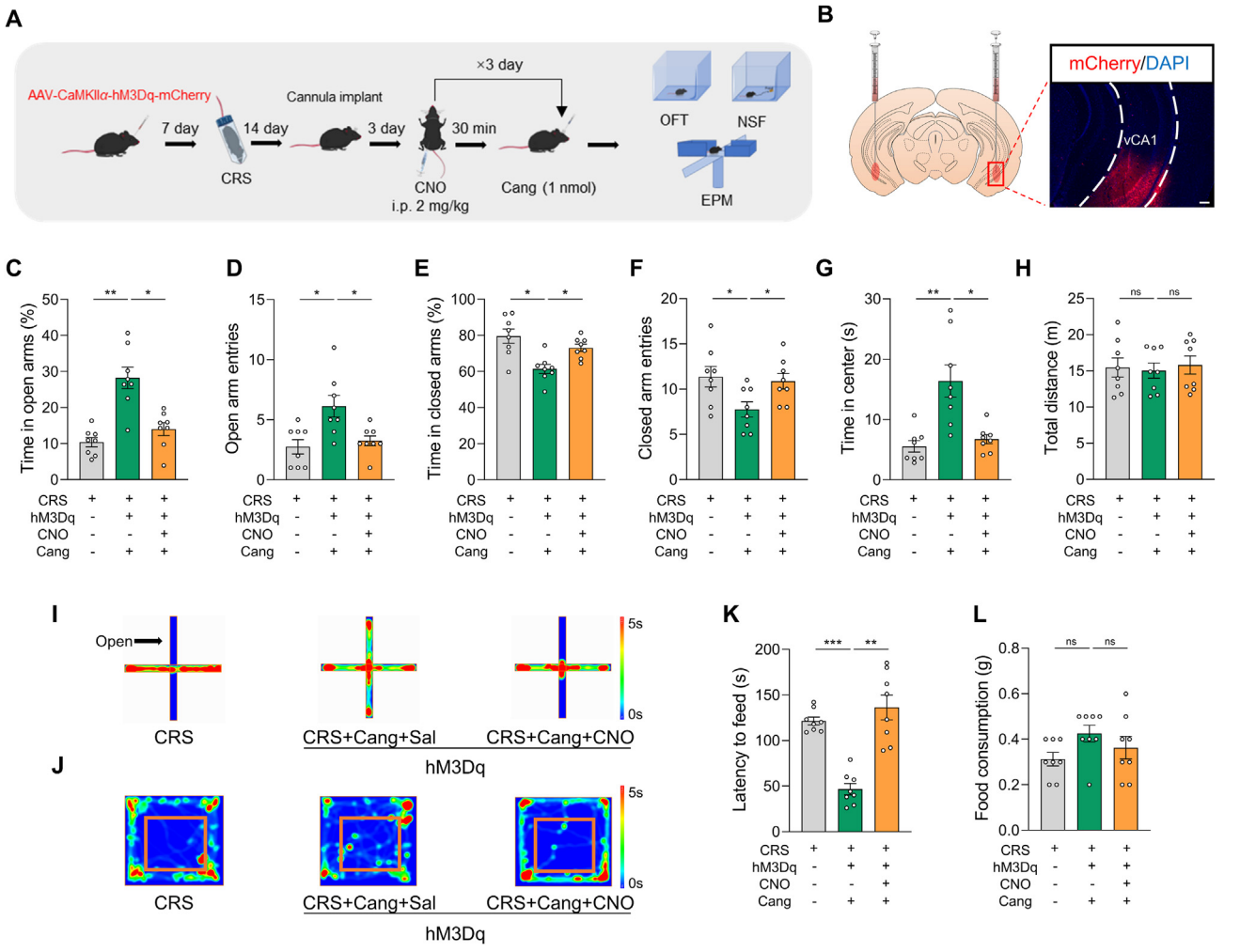

Figure 9 GPR17 modulates anxiety-like behaviors *via* BLA to vCA1 glutamatergic projection. (A) Experimental procedures. (B) Schematic and representative images of viral injection site and expression in vCA1. Scale bar = 100 μm. Statistic data of time in open arms (C), open arm entries (D), time in closed arms (E) and closed arm entries (F) in EPM test ($n = 8$). Statistic data of time in center (G) and total distance (H) in OFT ($n = 8$). Heatmap-plot in EPM test (I) and OFT (J). Statistic data of latency to feed (K) and food consumption (L) in NSF test ($n = 8$). All data are expressed as the mean ± SEM. ns $P > 0.05$; *$P < 0.05$; **$P < 0.01$; ***$P < 0.001$.

mice entered the open arms in EPM test and after behavioral tests. More importantly, these were reversed by cangrelor, which had an inhibitory effect on GPR17[48,49]. Furthermore, chemogenetic activation of BLA glutamatergic neuron activity reversed the anxiolytic-like effects of cangrelor. These indicate that GPR17 plays an important role in anxiety-like behaviors by regulating the BLA glutamatergic neuronal activity. It has been reported that GPR17 is activated by nucleotide sugars and cysteinyl leukotrienes, involving in the activation of desensitization machinery which started with phosphorylation of agonist-activated receptor by second messenger-dependent and/or GPCR kinases (GRKs). Agonist-triggered phosphorylation of GPCRs by GRKs primes the recruitment of the regulatory proteins β-arrestins[7,50]. It is indeed known that β-arrestins play an important role in GPCR signaling. They serve both to terminate G protein-dependent signals and confer novel intracellular properties to the receptor, by acting as adaptors or scaffolds for other signaling proteins, such as signal-regulated kinases

Schematic of virus injection, cannula implanted to inject cangrelor or saline for 3 consecutive days and fiber implanted into vCA1 to record Ca^{2+} signals (top). Representative image of fiber site in vCA1 (bottom). Scale bar = 100 μm. (L) Representative heatmap-plot and averaged traces of normalized Ca^{2+} fluorescence ($\Delta F/F$) ± SEM (shades) in vCA1 PyNs. Time 0 is defined as the moment the mouse entered open arms in EPM test. (M) Statistical data of area under curve in vCA1 PyNs ($n = 6$). (N) Schematic of virus injection, cannulas implanted to inject cangrelor or saline for 3 consecutive days, and fiber implanted into vCA1 to record glutamate signals (top). Representative image of fiber site in vCA1 (bottom). Scale bar = 100 μm. (O) Representative heatmap-plot and averaged traces of normalized glutamate fluorescence ($\Delta F/F$) ± SEM (shades) in vCA1. Time 0 is defined as the moment the mouse entered open arms in EPM test. (P) Statistical data of area under curve in vCA1 neurons ($n = 6$). All data are expressed as the mean ± SEM. *$P < 0.05$; **$P < 0.01$; ***$P < 0.001$.

(ERKs)[7,51]. As substrates for ERK, potassium (K^+) channels, which are mainly composed of KCNQ2 and KCNQ3 subunits, are phosphorylated by ERK and slowly inactivated in the nervous system[52]. Therefore, we speculated that downregulation of GPR17 could inhibit the GRKs/β-arrestins/ERKs pathway, activate K^+ channels, reduce firing rate of action potential and hence decrease the glutamatergic neuronal activity. The mechanism of GPR17 regulating neuronal activity will be investigated in our future studies.

The BLA is a vital site that regulates emotional processes and BLA dysfunction is regarded as a direct responsory to regulate anxiety-like behaviors[53]. BLA neurons emit neural projections to multiple brain regions. We have used viral tracing techniques to find that infralimbic cortex, prelimbic cortex, bed nucleus of stria terminalis, dorsal and ventral hippocampus and lateral septal nucleus receive projections from the BLA glutamatergic neurons. However, only the activity of vCA1 PyNs had a significant enhancement in CRS mice and was reversed by cangrelor. These suggest that GPR17 is involved in regulating anxiety-like behaviors through the BLA glutamatergic neuronal projection to vCA1 PyNs. The ventral hippocampus is one of the major brain regions responsible for regulating mood and emotion. It has been reported that activation of the BLA to ventral hippocampus circuit obviously aggravated anxiety-related behaviors[47,54]. In our study, we confirmed the BLA to vCA1 glutamatergic projection. We found the axonal calcium signals of BLA fibers in vCA1 and the glutamate release in vCA1 undergo similar fluctuations to those in BLA, and these were also regulated by GPR17. What's more, activation of BLA to vCA1 glutamatergic projection blocked the anxiolytic-like effects of the GPR17 antagonist. These identify GPR17 regulates anxiety-like behaviors through BLA to vCA1 glutamatergic projection.

5. Conclusions

Taken together, our study finds for the first and highlights the new function of GPR17 in regulating anxiety-like behaviors. GPR17 in BLA glutamatergic neurons participates in the etiopathogenesis of anxiety disorders through BLA to vCA1 glutamatergic projection, and it might be a novel potential target for the treatment of anxiety disorders. Our research may enrich the pathogenesis of anxiety disorders and provide new information for the potential therapeutic targets for anxiety disorders.

Acknowledgements

This work was supported by grants from the National Natural Science Foundation of China (82373860 and 82071202 to Susu Tang, 82173805 to Hao Hong) and National Innovation and Entrepreneurship Training Program for Undergraduate (202410316198, China).

Author contributions

Ruizhe Nie: Investigation, Visualization, Data curation, Writing-Original Draft, Writing-review & editing. Xinting Zhou: Investigation, Methodology. Jiaru Fu: Investigation. Shanshan Hu: Investigation, Visualization. Qilu Zhang: Investigation. Weikai Jiang: Investigation. Yizi Yan: Investigation. Xian Cao: Investigation. Danhua Yuan: Investigation. Yan Long: Visualization. Hao Hong: Resources, Supervision, Funding acquisition. Susu Tang: Conceptualization, Project administration, Supervision, Funding acquisition, Writing-Original Draft, Writing-review & editing.

Conflicts of interest

The authors declare no conflicts of interest.

Appendix A. Supporting information

Supporting information to this article can be found online at https://doi.org/10.1016/j.apsb.2024.08.005.

References

1. Craske MG, Stein MB. Anxiety. *Lancet* 2016;**388**:3048−59.
2. Szuhany KL, Simon NM. Anxiety disorders: a review. *JAMA* 2022;**328**:2431−45.
3. Zhang K, Chen L, Yang J, Liu J, Li J, Liu Y, et al. Gut microbiota-derived short-chain fatty acids ameliorate methamphetamine-induced depression- and anxiety-like behaviors in a Sigmar-1 receptor-dependent manner. *Acta Pharm Sin B* 2023;**13**:4801−22.
4. Penninx BW, Pine DS, Holmes EA, Reif A. Anxiety disorders. *Lancet* 2021;**397**:914−27.
5. Benned-Jensen T, Rosenkilde MM. Distinct expression and ligand-binding profiles of two constitutively active GPR17 splice variants. *Br J Pharmacol* 2010;**159**:1092−105.
6. Ciana P, Fumagalli M, Trincavelli ML, Verderio C, Rosa P, Lecca D, et al. The orphan receptor GPR17 identified as a new dual uracil nucleotides/cysteinyl-leukotrienes receptor. *EMBO J* 2006;**25**:4615−27.
7. Daniele S, Trincavelli ML, Fumagalli M, Zappelli E, Lecca D, Bonfanti E, et al. Does GRK-β arrestin machinery work as a "switch on" for GPR17-mediated activation of intracellular signaling pathways?. *Cell Signal* 2014;**26**:1310−25.
8. Tang SS, Hong H, Chen L, Mei ZL, Ji MJ, Xiang GQ, et al. Involvement of cysteinyl leukotriene receptor 1 in Aβ_{1-42}-induced neurotoxicity *in vitro* and *in vivo*. *Neurobiol Aging* 2014;**35**:590−9.
9. Tang SS, Wang XY, Hong H, Long Y, Li YQ, Xiang GQ, et al. Leukotriene D4 induces cognitive impairment through enhancement of CysLT$_1$ R-mediated amyloid-β generation in mice. *Neuropharmacology* 2013;**65**:182−92.
10. Chen F, Ghosh A, Lin J, Zhang C, Pan Y, Thakur A, et al. 5-Lipoxygenase pathway and its downstream cysteinyl leukotrienes as potential therapeutic targets for Alzheimer's disease. *Brain Behav Immun* 2020;**88**:844−55.
11. Lin JR, Fang SC, Tang SS, Hu M, Long Y, Ghosh A, et al. Hippocampal CysLT$_1$R knockdown or blockade represses LPS-induced depressive behaviors and neuroinflammatory response in mice. *Acta Pharmacol Sin* 2017;**38**:477−87.
12. Liu X, Tang SS, Liu SM, Zeng J, Chen ZG, Liu CH, et al. Deficiency of astrocyte CysLT$_1$R ameliorates depression-like behaviors in mice by modulating glutamate synaptic transmission. *Neurobiol Dis* 2022;**175**:105922.
13. Marucci G, Dal Ben D, Lambertucci C, Martí Navia A, Spinaci A, Volpini R, et al. GPR17 receptor modulators and their therapeutic implications: review of recent patents. *Expert Opin Ther Pat* 2019;**29**:85−95.
14. Wang J, He X, Meng H, Li Y, Dmitriev P, Tian F, et al. Robust myelination of regenerated axons induced by combined manipulations of GPR17 and microglia. *Neuron* 2020;**108**:876−86.e4.
15. Merten N, Fischer J, Simon K, Zhang L, Schröder R, Peters L, et al. Repurposing HAMI3379 to block GPR17 and promote rodent and human oligodendrocyte differentiation. *Cell Chem Biol* 2018;**25**:775−886.e5.
16. Fumagalli M, Daniele S, Lecca D, Lee PR, Parravicini C, Fields RD, et al. Phenotypic changes, signaling pathway, and functional correlates

of GPR17-expressing neural precursor cells during oligodendrocyte differentiation. *J Biol Chem* 2011;**286**:10593−604.
17. Seyedsadr MS, Ineichen BV. Gpr17, a player in lysolecithin-induced demyelination, oligodendrocyte survival, and differentiation. *J Neurosci* 2017;**37**:2273−5.
18. Dziedzic A, Miller E, Saluk-Bijak J, Bijak M. The GPR17 receptor-a promising goal for therapy and a potential marker of the neurodegenerative process in multiple sclerosis. *Int J Mol Sci* 2020;**21**:1852.
19. Nyamoya S, Leopold P, Becker B, Beyer C, Hustadt F, Schmitz C, et al. G-protein-coupled receptor Gpr17 expression in two multiple sclerosis remyelination models. *Mol Neurobiol* 2019;**56**:1109−23.
20. Fumagalli M, Lecca D, Coppolino GT, Parravicini C, Abbracchio MP. Pharmacological properties and biological functions of the GPR17 receptor, a potential target for neuro-regenerative medicine. *Adv Exp Med Biol* 2017;**1051**:169−92.
21. Bonfanti E, Gelosa P, Fumagalli M, Dimou L, Viganò F, Tremoli E, et al. The role of oligodendrocyte precursor cells expressing the GPR17 receptor in brain remodeling after stroke. *Cell Death Dis* 2017;**8**:e2871.
22. Ceruti S, Villa G, Genovese T, Mazzon E, Longhi R, Rosa P, et al. The P2Y-like receptor GPR17 as a sensor of damage and a new potential target in spinal cord injury. *Brain* 2009;**132**:2206−18.
23. Mao FX, Chen HJ, Qian LH, Buzby JS. GPR17 plays a role in ischemia-induced endogenous repair of immature neonatal cerebral White matter. *Brain Res Bull* 2020;**161**:33−42.
24. Zhao B, Wang H, Li CX, Song SW, Fang SH, Wei EQ, et al. GPR17 mediates ischemia-like neuronal injury *via* microglial activation. *Int J Mol Med* 2018;**42**:2750−62.
25. Zhao B, Zhao CZ, Zhang XY, Huang XQ, Shi WZ, Fang SH, et al. The new P2Y-like receptor G protein-coupled receptor 17 mediates acute neuronal injury and late microgliosis after focal cerebral ischemia in rats. *Neuroscience* 2012;**202**:42−57.
26. Franke H, Parravicini C, Lecca D, Zanier ER, Heine C, Bremicker K, et al. Changes of the GPR17 receptor, a new target for neurorepair, in neurons and glial cells in patients with traumatic brain injury. *Purinergic Signal* 2013;**9**:451−62.
27. Lecca D, Trincavelli ML, Gelosa P, Sironi L, Ciana P, Fumagalli M, et al. The recently identified P2Y-like receptor GPR17 is a sensor of brain damage and a new target for brain repair. *PLoS One* 2008;**3**:e3579.
28. Shao LX, Jiang Q, Liu XX, Gong DM, Yin YX, Wu G, et al. Functional coupling of Tmem74 and HCN1 channels regulates anxiety-like behavior in BLA neurons. *Mol Psychiatry* 2019;**24**:1461−77.
29. Luo ZY, Huang L, Lin S, Yin YN, Jie W, Hu NY, et al. Erbin in Amygdala parvalbumin-positive neurons modulates anxiety-like behaviors. *Biol Psychiatry* 2020;**87**:926−36.
30. Yan L, Wei JA, Yang F, Wang M, Wang S, Cheng T, et al. Physical exercise prevented stress-induced anxiety *via* improving brain RNA methylation. *Adv Sci* 2022;**9**:e2105731.
31. Liu WZ, Zhang WH, Zheng ZH, Zou JX, Liu XX, Huang SH, et al. Identification of a prefrontal cortex-to-amygdala pathway for chronic stress-induced anxiety. *Nat Commun* 2020;**11**:2221.
32. Qi G, Zhang P, Li T, Li M, Zhang Q, He F, et al. NAc-VTA circuit underlies emotional stress-induced anxiety-like behavior in the three-chamber vicarious social defeat stress mouse model. *Nat Commun* 2022;**13**:577.
33. Avery SN, Clauss JA, Blackford JU. The human BNST: functional role in anxiety and addiction. *Neuropsychopharmacology* 2016;**41**:126−41.
34. Gairing SJ, Galle PR, Schattenberg JM, Kostev K, Labenz C. Portal vein thrombosis is associated with an increased incidence of depression and anxiety disorders. *J Clin Med* 2021;**10**:5689.
35. Qin Z, Zhou X, Pandey NR, Vecchiarelli HA, Stewart CA, Zhang X, et al. Chronic stress induces anxiety *via* an amygdalar intracellular cascade that impairs endocannabinoid signaling. *Neuron* 2015;**85**:1319−31.
36. Sah P. Fear, anxiety, and the amygdala. *Neuron* 2017;**96**:1−2.
37. Pang L, Zhu S, Ma J, Zhu L, Liu Y, Ou G, et al. Intranasal temperature-sensitive hydrogels of cannabidiol inclusion complex for the treatment of post-traumatic stress disorder. *Acta Pharm Sin B* 2021;**11**:2031−47.
38. Ferri J, Eisendrath SJ, Fryer SL, Gillung E, Roach BJ, Mathalon DH. Blunted amygdala activity is associated with depression severity in treatment-resistant depression. *Cogn Affect Behav Neurosci* 2017;**17**:1221−31.
39. Sah P, Faber ES, Lopez De Armentia M, Power J. The amygdaloid complex: anatomy and physiology. *Physiol Rev* 2003;**83**:803−34.
40. Hájos N. Interneuron types and their circuits in the basolateral Amygdala. *Front Neural Circuits* 2021;**15**:687257.
41. Cao J, Liu X, Liu JX, Zhao S, Guo YX, Wang GY, et al. Inhibition of glutamatergic neurons in layer II/III of the medial prefrontal cortex alleviates paclitaxel-induced neuropathic pain and anxiety. *Eur J Pharmacol* 2022;**936**:175351.
42. Zhang GW, Shen L, Tao C, Jung AH, Peng B, Li Z, et al. Medial preoptic area antagonistically mediates stress-induced anxiety and parental behavior. *Nat Neurosci* 2021;**24**:516−28.
43. Abdul M, Yan HQ, Zhao WN, Lyu XB, Xu Z, Yu XL, et al. VTA-NAc glutaminergic projection involves in the regulation of pain and pain-related anxiety. *Front Mol Neurosci* 2022;**15**:1083671.
44. Liu J, Li D, Huang J, Cao J, Cai G, Guo Y, et al. Glutamatergic neurons in the amygdala are involved in paclitaxel-induced pain and anxiety. *Front Psychiatry* 2022;**13**:869544.
45. Jones SK, McCarthy DM, Vied C, Stanwood GD, Schatschneider C, Bhide PG. Transgenerational transmission of aspartame-induced anxiety and changes in glutamate-GABA signaling and gene expression in the amygdala. *Proc Natl Acad Sci U S A* 2022;**119**:e2213120119.
46. Zhang JY, Liu TH, He Y, Pan HQ, Zhang WH, Yin XP, et al. Chronic stress remodels synapses in an Amygdala Circuit-specific manner. *Biol Psychiatry* 2019;**85**:189−201.
47. Felix-Ortiz AC, Beyeler A, Seo C, Leppla CA, Wildes CP, Tye KM. BLA to vHPC inputs modulate anxiety-related behaviors. *Neuron* 2013;**79**:658−64.
48. Ren H, Orozco IJ, Su Y, Suyama S, Gutiérrez-Juárez R, Horvath TL, et al. FoxO1 target Gpr17 activates AgRP neurons to regulate food intake. *Cell* 2012;**149**:1314−26.
49. Coppi E, Maraula G, Fumagalli M, Failli P, Cellai L, Bonfanti E, et al. UDP-glucose enhances outward K^+ currents necessary for cell differentiation and stimulates cell migration by activating the GPR17 receptor in oligodendrocyte precursors. *Glia* 2013;**61**:1155−71.
50. Gurevich EV, Tesmer JJ, Mushegian A, Gurevich VV. G protein-coupled receptor kinases: more than just kinases and not only for GPCRs. *Pharmacol Ther* 2012;**133**:40−69.
51. Zheng H, Loh HH, Law PY. β-Arrestin-dependent μ-opioid receptor-activated extracellular signal-regulated kinases (ERKs) translocate to nucleus in contrast to G protein-dependent ERK activation. *Mol Pharmacol* 2008;**73**:178−90.
52. Brown DA, Passmore GM. Neural KCNQ (Kv7) channels. *Br J Pharmacol* 2009;**156**:1185−95.
53. Daviu N, Bruchas MR, Moghaddam B, Sandi C, Beyeler A. Neurobiological links between stress and anxiety. *Neurobiol Stress* 2019;**11**:100191.
54. Deji C, Yan P, Ji Y, Yan X, Feng Y, Liu J, et al. The basolateral amygdala to ventral hippocampus circuit controls anxiety-like behaviors induced by morphine withdrawal. *Front Cel Neurosci* 2022;**16**:894886.